ACS OMEGA

http://pubs.acs.org/journal/acsodf

Article

Kinetic Study on High-Temperature H_2S Removal over Mn-Based Regenerable Sorbent Using Deactivation Model

Ju Wang, Jie Xu, Xianli Wu, Bin Liang, and Chunhua Du*

Cite This: *ACS Omega* 2022, 7, 2718−2724

Read Online

ACCESS | Metrics & More | Article Recommendations | Supporting Information

ABSTRACT: The kinetics of high-temperature H_2S removal over Mn/Al sorbents prepared by co-precipitation method was investigated in a fixed-bed reactor using a deactivation model. The initial sorption rate constant (k_0), deactivation rate constant (k_d), apparent activation energy (E_a), and deactivation energy (E_d) were obtained. The k_0 and k_d values of Mn/Al sorbents are much higher than those of pure Mn_2O_3. This indicates that Mn/Al sorbents have higher reactivity on the removal of H_2S and less diffusion resistance caused by the formation of the sulfided product. The E_a and E_d values for the sorbent with the Mn content (wt %) of 35.4% are 38.18 and 31.05 kJ/mol, respectively. The deactivation model gives excellent predictions for the H_2S breakthrough curves in the sulfidation−regeneration process.

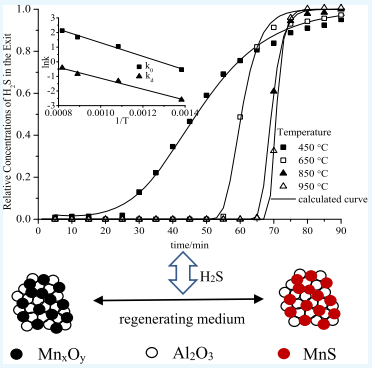

1. INTRODUCTION

The removal of H_2S from syngas produced in the gasification of coal, biomass, municipal solid waste, and so forth is an essential step in the processes using syngas as feedstocks or fuels, in which H_2S may cause severe corrosion of downstream equipment as well as sulfur oxide emission.[1−3] The currently commercial desulfurization process uses an amine solution to absorb sulfur hydride for the syngas at near-ambient temperature.[4−7] This process leads to substantial thermal efficiency loss on account of the cooling-down and heating-up of hot syngas.

Hot gas desulfurization with metal oxide sorbents has been widely investigated in the past few decades. The sorbents containing zinc,[8,9] ferric,[10,11] or copper[12−14] have been extensively reported for hot gas desulfurization. However, these metal oxides could only work effectively at temperatures of <600 °C because they are prone to be reduced into a metallic state or form metal carbides at higher temperatures.

Mn-based sorbents have been developed, and they showed high sulfur capacity, high mechanical stability, high thermal stability, and fast initial reaction rate for H_2S removal at 850 °C which is close to the gasifier temperature.[15−20] To attain a high thermal efficiency, sulfur removal at a high temperature is the most preferable choice. On the other hand, high-temperature desulfurization might lead to additional large savings because the heat exchange equipment is omitted.[21] In our earlier work,[22] Mn/Al sorbents were prepared by a co-precipitation method for 850 °C H_2S removal. We found that the used sorbents could be easily regenerated by diluted air or steam. The performance of these sorbents appeared to be stable over multiple cycles, which may meet the requirements of high-temperature desulfurization.

In order to scale up and commercialize hot coal gas desulfurization, the kinetic analysis of H_2S removal should be investigated. The removal of H_2S with metal oxide sorbents is a typical noncatalytic gas−solid reaction. Many kinetic models have been proposed to describe the kinetics, such as the unreacted shrinking core model (SCM),[23] deactivation model (DM),[24] deactivation kinetic model (DKM),[25,26] and so forth. The SCM assumes that the reaction occurs at a sharp interface between the reacted outer surface and the unreacted interior core. It is suitable for solid sorbents with low porosity. The DM is reported to be successful in predicting the conversion−time data for gas−solid reactions. To modify the DM, Yasyerli et al.[27−29] introduced the concentration dependence of the deactivation term and applied it to describe the removal of H_2S over a variety of sorbents, which has excellent predictions for the H_2S breakthrough curves. Hong et al.[25,26] hold the view that the DM model is not suitable for all complicated desulfurization reactions because the reaction order of H_2S and the sorbent is assumed to be 1. They established the DKM based on the elementary stoichiometric equation of the desulfurization reaction. In earlier works,[23,30] it was found

Received: September 21, 2021
Accepted: December 28, 2021
Published: January 10, 2022

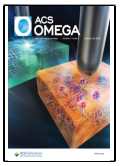

https://doi.org/10.1021/acsomega.1c05243
ACS Omega 2022, 7, 2718−2724

that the reaction order of H_2S and Mn-based sorbents is 1, which is in accordance with the assumption of Yasyerli.[27−29]

In this work, we focus on the kinetic behaviors of the Mn/Al sorbents prepared by the co-precipitation method. The activity and regenerability of the Mn/Al sorbents were tested in a fixed-bed reactor, and the sorption rate parameters were evaluated by the analysis of the H_2S breakthrough curves using the DM modified by Yasyerli. This work is essential for the scale-up and commercialization of high-temperature desulfurization using a Mn-based regenerable sorbent.

2. DEACTIVATION MODEL

In the removal of H_2S, significant changes in the pore structure, active surface area, and activity per unit area of the sorbent have been caused by the formation of a dense product layer with the reaction extent. DM has not considered the detailed characteristic parameters of the solid sorbent in such a microscopic way as SCM but in a macroscopic way. In the DM, the effects of the textural variation (pore structure, active surface area, and activity per unit area) of the sorbent and an additional diffusion resistance caused by the formation of the dense product layer were combined in an activity term. The change in the rate of the activity of the sorbent was written as

$$-\frac{da}{dt} = k_d C a \tag{1}$$

where k_d is the deactivation rate constant. With the pseudo-steady-state assumption, the species conservation equation for the reactant gas H_2S in a fixed-bed reactor was expressed as

$$-Q\frac{dC}{dW} = k_0 C a \tag{2}$$

where k_0 is the initial reaction rate constant. The following equation for the H_2S breakthrough curves was then derived by an iterative procedure.

$$\frac{C}{C_0} = \exp\left\{\frac{\left[1 - \exp\left(\frac{k_0 W}{Q}(1 - \exp(-k_d t))\right)\right]}{[1 - \exp(-k_d t)]}\exp(-k_d t)\right\} \tag{3}$$

The rate constants k_d and k_0 can be evaluated by the regression analysis of the H_2S breakthrough curve.

3. RESULTS AND DISSCUSSION

3.1. H_2S Sorption Results with Mn/Al Sorbents with Different Mn Contents. The H_2S breakthrough data over the sorbents with different Mn contents at 850 °C and the breakthrough curves predicted by DM are presented in Figure 1. In the initial period, the outlet H_2S concentration is lower than the detection limits of GC, and the removal ratios of H_2S of all sorbents are essentially 100%. Mn oxides could reduce H_2S from 1% to <5 ppm at 850 °C. As the Mn content increased, the breakthrough curves shift to longer times, indicating a higher sorption capacity. As shown in Table 1, the sulfur capacity of the sorbent increases with an increase in the Mn content. The S/Mn molar ratios of all the saturated sorbents are between 0.88 and 0.96, indicating the approximate utilization ratio of the active component.

For samples 1−4, regression analyses of the kinetic model are of good agreement with the experimental data, and the breakthrough curves are all very sharp. The obtained correlative coefficients (R^2) listed in Table 1 are close to 1.

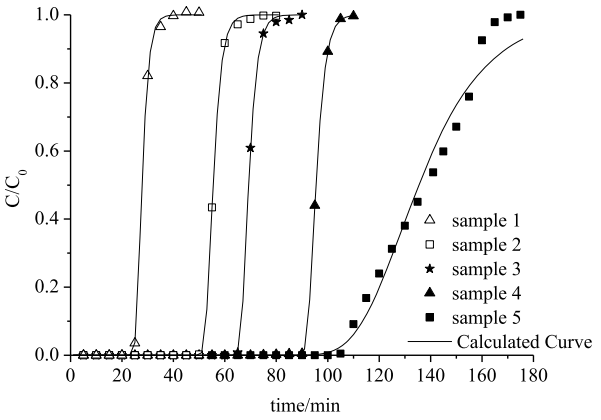

Figure 1. Experimental data and calculated H_2S breakthrough curves for samples with different Mn contents; T = 850 °C; GHSV = 11 942 h^{-1}.

For sample 5, pure Mn_2O_3, the curve has a significant tail in the breakthrough period, and the completion of the breakthrough curve takes quite some time.

The rate parameters evaluated from the kinetic model are listed in Table 1. For samples 1−4, the deactivation rate constants k_d range from 0.5579 to 0.3962 min^{-1}, which are of the same order of magnitude. The initial reaction rate constants k_0 increase from 2.7363 to 6.7697 $m^3 \cdot kg^{-1} \cdot min^{-1}$ when the Mn content increases from 13.7 to 46.5%. The k_0 values obtained with sample 3 and sample 4 are higher than the corresponding values reported with the Zn−Mn (4.36 $m^3 \cdot kg^{-1} \cdot min^{-1}$), V−Mn (4.04 $m^3 \cdot kg^{-1} \cdot min^{-1}$), and Fe−Mn (3.31 $m^3 \cdot kg^{-1} \cdot min^{-1}$) sorbents.[27] The initial reaction rate constant k_0 is closely correlated with the diffusion resistance of H_2S molecules, and the active sites reacted with H_2S. For the supported sorbents prepared by the sol−gel or impregnation method, the rate constants often decline with the increase of active species because the specific surface or active sites on the surface decreased with the incremental loading amount of metal oxide.[25] However, for sorbents prepared by the co-precipitation method in this work, a good dispersion of Mn−Al in bulk phase is achieved. With the increase of Mn content, the diffusion resistance of H_2S molecules in Mn−Al sorbents declines and the number of active sites that reacted with H_2S rises.

For sample 5, pure Mn_2O_3, k_d is 1 order of magnitude lower than those of samples 1−4, and k_0 is the lowest, which indicates the significant increase of diffusion resistance caused by the formation of the sulfided product.

3.2. Effect of GHSV on Desulfurization Reaction over Mn/Al Sorbent. A set of sulfidation tests was conducted over sample 3 with different flow rates ranging from 50 to 125 mL/min. The corresponding GHSVs range from 11 942 to 29 855 h^{-1}. Figure 2 shows the experimental data obtained with different GHSVs and the breakthrough curves predicted by DM. It could be seen that the breakthrough curves calculated using the kinetic model are almost identical with the experimental data.

The sulfur capacities and the results of regression analysis are shown in Table 2. The sulfur capacity almost keeps stable at different GHSVs, indicating that external mass-transfer resistances can be neglected within the ranges of 11 942−29 855 h^{-1} at 850 °C. Both the deactivation rate constant k_d and the initial reaction rate constant k_0 do not depend on GHSV.

https://doi.org/10.1021/acsomega.1c05243
ACS Omega 2022, 7, 2718−2724

Table 1. Rate Parameters Evaluated from the Breakthrough Data for Samples with Different Mn Contents

samples	1	2	3	4	5
k_d (min^{-1})	0.5579	0.4404	0.4350	0.3962	0.0554
k_0 ($m^3 \cdot kg^{-1} \cdot min^{-1}$)	2.7363	4.3460	5.3797	6.7697	1.2907
R^2	0.9997	0.9998	0.9999	1.0000	0.9881
sulfur capacity (g S/100 g sorbent)	7	15	18	25	36
S/Mn molar ratio	0.88	0.96	0.92	0.92	0.89

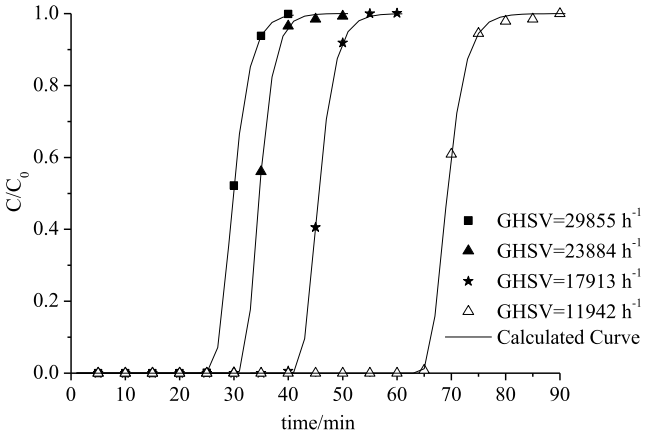

Figure 2. Experimental data and the calculated H_2S breakthrough curves for sample 3 at different GHSVs (h^{-1}); T = 850 °C.

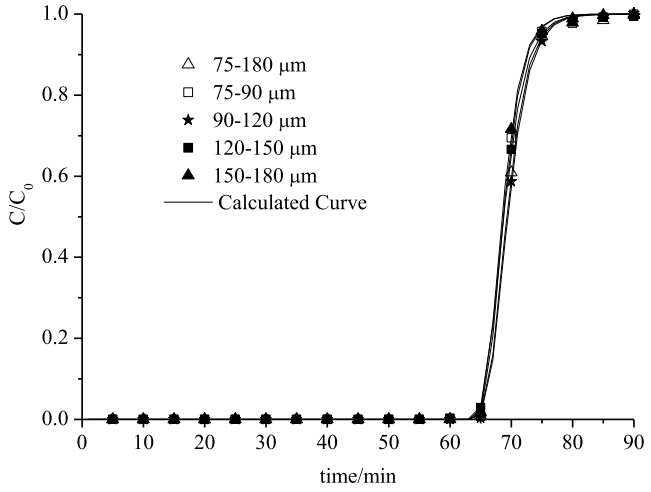

Figure 3. Experimental data and the calculated H_2S breakthrough curves for sample 3 with different particle sizes; T = 850 °C; GHSV = 11 942 h^{-1}.

The R^2 values are all higher than the critical values, which means that all regressions are significant.[31]

As expected, the breakthrough time becomes shorter with increased GHSV, whereas the outlet H_2S concentration before breakthrough is lower than the detection limits of GC at all GHSVs, and the sulfur capacity almost maintains constant. From the viewpoint of industrialization, it is favorable for the extensive output to increase GHSV.

3.3. Effects of Particle Size on Desulfurization Reaction over Sample 3. To investigate the effects of internal diffusion on H_2S removal,[32] another set of experiments was carried out over sample 3 with different particle sizes in the range of 80−200 mesh. Figure 3 shows the data obtained in the desulfurization reaction and the breakthrough curves predicted by DM. The rate parameters evaluated from the kinetic model are listed in Table 3. In the particle size of 80−200 mesh (75−180 μm), the breakthrough curves coincide well. Further, the rate constants k_d and k_0 do not show significant changes. The internal diffusion is considered to have little effects in this range of particle size.

3.4. Effects of Temperature on Desulfurization Reaction and Estimation of Activation Energies. Sample 3 was sulfided at different temperatures ranging from 450−950 °C. Figure 4 shows the experimental data and the calculated H_2S breakthrough curves related to the desulfurization reaction temperature. The evaluated rate parameters and sulfur capacities at different temperatures are listed in Table 4.

As shown in Figure 4, the breakthrough time at 450 °C is the shortest, and the sulfur capacity decreases to 13 g S/100 g sorbent. Furthermore, the relative concentrations of H_2S before breakthrough at 450 °C are between 0.009 and 0.019 (85−150 ppm), as seen in the magnified patterns of Figure 4. It is commonly believed that Mn oxides can reduce the amount of H_2S to a level below 50 ppm at 400−1000 °C.[21] However, the Mn/Al sorbents prepared by the co-precipitation method have less surface active sites than those prepared by impregnation, which have a negative effect on the desulfurization performance at mid-temperature. With the increase of temperature, O/S exchange penetrates into the bulk phase of the sorbent because of the increase of the solid-state diffusion rate. The desulfurization efficiency and the sulfur capacity improve. At temperatures from 650 to 950 °C, the initial H_2S concentrations are lower than the detection limits of GC, and the sulfur capacities increase from 16 to 18 g S/100 g sorbent. Mn/Al sorbents prepared by the co-precipitation method are suitable for high-temperature desulfurization.

As expected, the data listed in Table 4 show that the rate constants increased with the temperature increase. The activation energies of the sorption rate constant and the deactivation rate constant can be calculated by linear regression of the Arrhenius equation. As shown in Figure 5,

Table 2. Sulfur Capacities and Rate Parameters Evaluated from the Breakthrough Data for Sample 3 at Different GHSVs (h^{-1})

$Q \times 10^6$ ($m^3 \cdot min^{-1}$)	50	75	100	125
GHSV (h^{-1})	11942	17913	23884	29855
k_d (min^{-1})	0.4350	0.4775	0.5484	0.4668
k_0 ($m^3 \cdot kg^{-1} \cdot min^{-1}$)	5.3797	5.8013	6.7450	6.1366
R^2	0.9999	1.0000	0.9999	1.0000
sulfur capacity (g S/100 g sorbent)	18	18	18	19

https://doi.org/10.1021/acsomega.1c05243
ACS Omega 2022, 7, 2718−2724

Table 3. Rate Parameters Evaluated from the Breakthrough Data for Sample 3 with Different Particle Sizes

mesh number	80−200	80−100	100−120	120−170	170−200
particle sizes (μm)	75−180	150−180	120−150	90−120	75−90
k_d (min^{-1})	0.4350	0.4832	0.4268	0.4245	0.4862
k_0 ($m^3 \cdot kg^{-1} \cdot min^{-1}$)	5.3797	5.9198	5.2399	5.2602	5.9727
R^2	0.9999	0.9999	1.0000	0.9999	0.9999

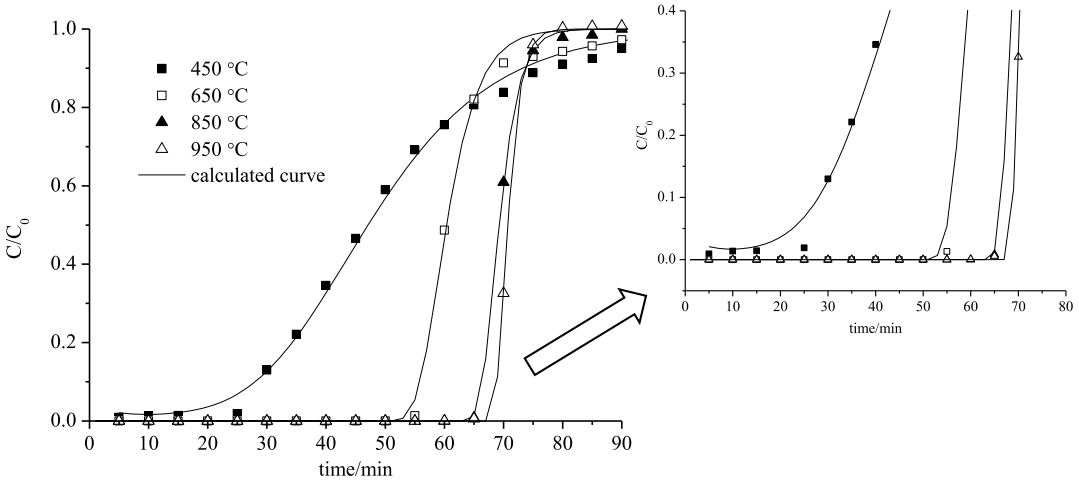

Figure 4. Experimental data and calculated H_2S breakthrough curves for sample 3 at different temperatures; GHSV = 11 942 h^{-1}.

Table 4. Rate Parameters and Sulfur Capacities Evaluated from the Breakthrough Data for Sample 3 at Different Temperatures

temperature (°C)	450	650	850	950
k_d (min^{-1})	0.0745	0.2676	0.4350	0.6646
k_0 ($m^3 \cdot kg^{-1} \cdot min^{-1}$)	0.5876	2.8551	5.3797	8.4316
R^2	0.9958	0.9985	0.9999	1.0000
sulfur capacity (g S/100 g sorbent)	13	16	18	18

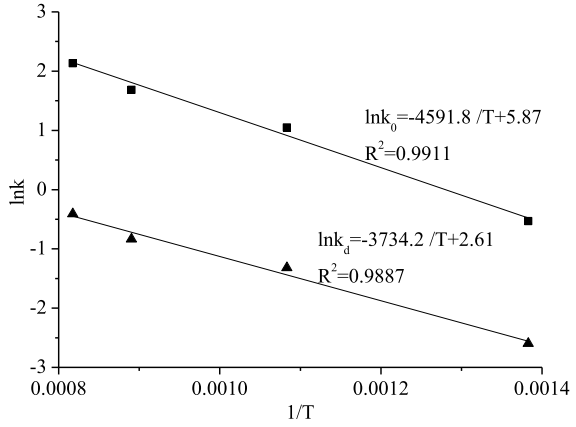

Figure 5. Plots of ln k_0 and ln k_d against $1/T$ for sample 3; GHSV = 11 942 h^{-1}.

the plots of ln k_0 and ln k_d against $1/T$ are almost linear. The obtained apparent activation energy (E_a) and deactivation energy (E_d) are 38.18 and 31.05 kJ/mol, respectively. These values are close to those of Cu_1Mn_9 mixed oxide/SBA-15 sorbents (33.02 and 46.34 kJ/mol) and those of La_3Mn_{97} mixed oxide/KIT-6 sorbents (48.98 and 56.10 kJ/mol) reported by Hong.[26] The obtained Arrhenius formulas of k_0 and k_d are expressed as follows

$$k_0 = 354.25 \exp(-38.18/RT) \quad (4)$$

$$k_d = 13.60 \exp(-31.05/RT) \quad (5)$$

where $R = 8.314 \times 10^{-3}$ kJ·mol^{-1}·k^{-1}, and T is the absolute temperature.

3.5. Rate Constants of the Sulfidation−Regeneration Process. Mn/Al sorbents can be regenerated completely with diluted air or steam. In this work, sample 3 was repeatedly sulfided and regenerated at 850 °C for five cycles using diluted air with 10% O_2 or using 81% H_2O in N_2 as the regenerating medium. It was found that DM has a good prediction ability for successive sulfidation.

Figure 6 shows the experimental data and calculated H_2S breakthrough curves of successive sulfidations during these tests. The calculated rate constants are listed in Table 5 and the changes of rate constants during the successive sulfidations are shown in Figure 7. It could be seen that the variation trends of k_0 and k_d are similar. Using 10% O_2 as the regenerating gas, k_0 and k_d were found to decline during the first three cycles, indicating an initial deactivation of this sorbent. In the next two cycles, k_0 and k_d are almost stable. The initial deactivation of Mn−Al sorbents has been observed by others for the samples prepared by the wet impregnation method.[33] The main reasons for the initial sorbent decay are proposed to be related to an alumina phase transition, the transformation of the Mn oxides, and the changes in textural properties.

Using 81% H_2O in N_2 as the regenerating gas, k_0 and k_d show no significant reduction. No deactivation was observed after five cycles. The reaction heat of regeneration with O_2 and steam at 1100 K is about −530 and −10.19 kJ/mol, respectively.[22] Thus, steam regeneration results in less sintering, which is related to the stabilization of rate constants.

4. CONCLUSIONS

The kinetic behavior for H_2S removal over Mn/Al sorbents in a fixed-bed reactor at a high temperature can be evaluated

https://doi.org/10.1021/acsomega.1c05243
ACS Omega 2022, 7, 2718−2724

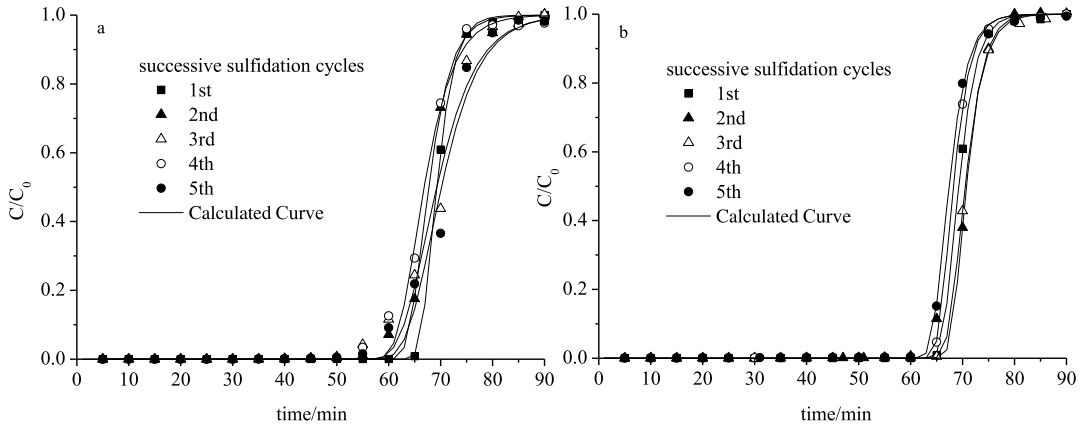

Figure 6. Experimental data and the calculated H_2S breakthrough curves in five cycles with (a) 10% O_2 or (b) 81% H_2O as the regenerating gas; T = 850 °C; GHSV = 11 942 h^{-1}.

Table 5. Rate Parameters Evaluated from the Breakthrough Data for Sample 3 at Successive Sulfidations

cycle number	1	2	3	4	5
k_d (min^{-1})	0.4350	(0.3360)[a]	(0.1913)	(0.2551)	(0.1987)
		0.4471	0.3981	0.4551	0.4125
k_0 ($m^3 \cdot kg^{-1} \cdot min^{-1}$)	5.3797	(4.0460)	(2.3290)	(3.0156)	(2.4539)
		5.6526	5.0075	5.5474	4.9599
R^2	0.9999	(0.9980)	(0.9889)	(0.9955)	(0.9890)
		0.9947	0.9999	0.9998	0.9998

[a]The data in parentheses are the rate constants for sample 3 regenerated with 10% O_2. Others are those for sample 3 regenerated with 81% H_2O.

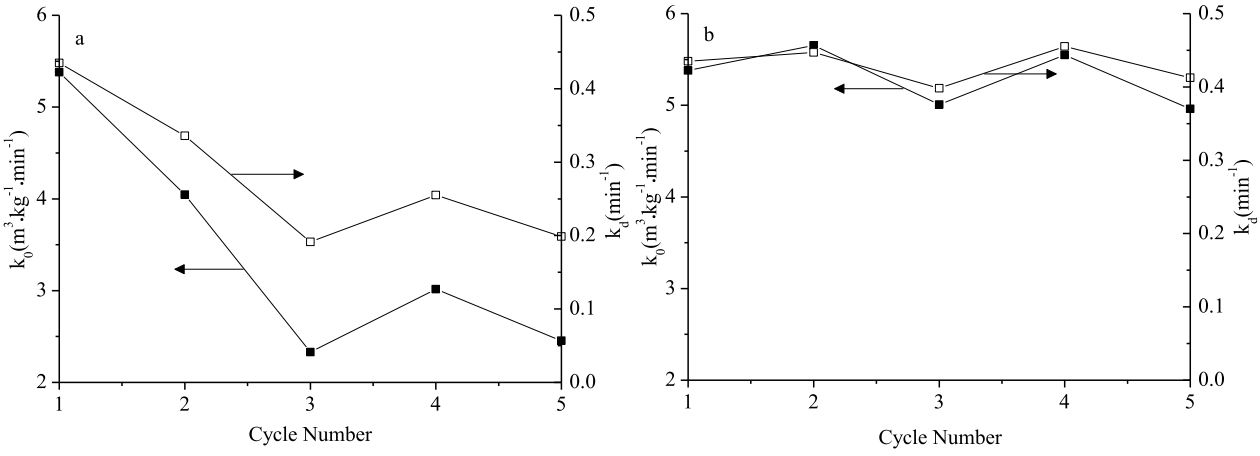

Figure 7. Relationship of the rate constants during five cycles with (a) 10% O_2 or (b) 81% H_2O as the regenerating gas; T = 850 °C; GHSV = 11 942 h^{-1}.

effectively by using the DM. The sorption rate constant (k_0), deactivation rate constant (k_d), apparent activation energy (E_a), and deactivation energy (E_d) were calculated. The k_0 and k_d values of the Mn/Al sorbent are much higher than those of pure Mn_2O_3. The E_a and E_d values for the sorbent with the Mn content (wt %) of 35.4% were 38.18 and 31.05 kJ/mol, respectively. The DM gives a good prediction for the experimental H_2S breakthrough data. It can be applied to the kinetic analysis of high-temperature H_2S removal over Mn-based sorbents without the requirement of the structural property of sorbents.

5. EXPERIMENTAL SECTION

5.1. Preparation of Sorbents. Five sorbents with different manganese contents were prepared by the co-precipitation method. 1.27 mol/L $Mn(NO_3)_2$ solution and 1 mol/L $Al(NO_3)_3$ solution were separately prepared from 50 wt % manganous nitrate solution (AR) and $Al(NO_3)_3 \cdot 9H_2O$ (AR). For samples 1, 2, 3, and 4, mixed nitrate solutions with different ratios of Mn/Al were neutralized with isovolumetric 10 wt % $NH_3 \cdot H_2O$. For sample 5, as a reference, pure Mn_2O_3 was prepared with 1.27 mol/L $Mn(NO_3)_2$ solution and isovolumetric 10 wt % $NH_3 \cdot H_2O$.

During precipitation, the nitrate solution and $NH_3 \cdot H_2O$ were simultaneously added into a reactor with a small amount of water. The pH value was kept in the range of 9−10, and the temperature was 50 °C. The precipitation slurry was aged at 50 °C for 2 h and then filtered and washed with distilled water. The filtration cake was dried, crushed, and sieved to the size of 80−200 mesh and then calcined at 850 °C in air for 6 h.

https://doi.org/10.1021/acsomega.1c05243
ACS Omega 2022, 7, 2718−2724

The Mn contents of the samples 1−5 were analyzed by the ammonium iron(II) sulfate titrimetric method (GB1506-2002-T), which are listed in Table 6. Each value is the average of three measurements. The absolute difference between the parallel measurements is not more than 1%.

Table 6. Measured Mn Content of Samples 1−5

sample	1	2	3	4	5
Mn content (wt %)	13.7	26.9	35.4	46.5	69.8

5.2. Sulfidation−Regeneration Tests. Sulfidation−regeneration tests were carried out in a fixed-bed reactor, which were described in detail in our previous works.[22,34] During the sulfidation stage, the sorbents were sulfided with a gas steam of 1% (15.179 g/m^3) H_2S in H_2 at 450−950 °C. The outlet H_2S concentration was measured by an SC2000 gas chromatograph (GC) which was equipped with a thermal conductivity detector and a flame photometric detector. The sulfidation ended when the H_2S concentration was close to that of the inlet gas.

The sulfided sorbents were regenerated with diluted air or steam. In the diluted air regeneration, the outlet gas contained SO_2 and elemental sulfur. Elemental sulfur was condensed after the reactor. The main product of steam regeneration is H_2S. The concentrations of SO_2 or H_2S were analyzed by GC. The regeneration stages were ended when the concentrations of SO_2 or H_2S were close to the detection limits of GC, which are 50 and 5 ppm, respectively. The regenerated acceptor was directly used for the sulfidation test in the next cycle.

Each experiment was repeated at least three times in sequence. The average values were reported. The amount of sulfur captured by the sorbents was evaluated by the numerical integration of the breakthrough curves.

■ ASSOCIATED CONTENT

Supporting Information

The Supporting Information is available free of charge at https://pubs.acs.org/doi/10.1021/acsomega.1c05243.

BET surface areas of fresh samples with different Mn contents and the experimental and regression data of C/C_0 (PDF)

■ AUTHOR INFORMATION

Corresponding Author

Chunhua Du − *College of Chemistry and Pharmaceutical Sciences, Qingdao Agricultural University, Qingdao 266109, China*; Phone: +86-532-58957922; Email: dch1218@163.com

Authors

Ju Wang − *College of Chemistry and Pharmaceutical Sciences, Qingdao Agricultural University, Qingdao 266109, China*; orcid.org/0000-0002-7540-9439

Jie Xu − *College of Chemistry and Pharmaceutical Sciences, Qingdao Agricultural University, Qingdao 266109, China*; orcid.org/0000-0002-0234-6342

Xianli Wu − *College of Chemistry and Pharmaceutical Sciences, Qingdao Agricultural University, Qingdao 266109, China*; orcid.org/0000-0002-8501-5548

Bin Liang − *College of Chemical Engineering, Sichuan University, Chengdu 610065, China*; orcid.org/0000-0003-2942-4686

Complete contact information is available at: https://pubs.acs.org/10.1021/acsomega.1c05243

Notes

The authors declare no competing financial interest.

■ ACKNOWLEDGMENTS

This work was supported by Science Foundation for the high-level talent of Qingdao Agricultural University (grant 6631114316 and 6631114350) and National Natural Science Foundation of China (grants 21706142 and 21346010).

■ NOMENCLATURE

a activity of the solid reactant
C outlet concentration of H_2S, g m^{-3}
C_0 inlet concentration of H_2S, g m^{-3}
k_d deactivation rate constant, min^{-1}
k_0 initial sorption rate constant, m^3 kg^{-1} min^{-1}
Q volumetric flow rate, m^3 min^{-1}
t time, min
W catalyst mass, kg

■ REFERENCES

(1) Yang, C.; Yang, S.; Fan, H.; Wang, Y.; Shangguan, J. Tuning the ZnO-activated carbon interaction through nitrogen modification for enhancing the H_2S removal capacity. *J. Colloid Interface Sci.* **2019**, *555*, 548−557.

(2) Daneshyar, A.; Ghaedi, M.; Sabzehmeidani, M. M.; Daneshyar, A. H_2S adsorption onto Cu-Zn−Ni nanoparticles loaded activated carbon and Ni-Co nanoparticles loaded γ-Al_2O_3: Optimization and adsorption isotherms. *J. Colloid Interface Sci.* **2017**, *490*, 553−561.

(3) Qi, J.; Wei, G.; Li, Y.; Li, J.; Sun, X.; Shen, J.; Han, W.; Wang, L. Porous carbon spheres for simultaneous removal of benzene and H_2S. *Chem. Eng. J.* **2018**, *339*, 499−508.

(4) Lin, Y.-H.; Chen, Y.-C.; Chu, H. The mechanism of coal gas desulfurization by iron oxide sorbents. *Chemosphere* **2015**, *121*, 62−67.

(5) Lee, J.; Feng, B. A thermodynamic study of the removal of HCl and H_2S from syngas. *Front. Chem. Sci. Eng.* **2012**, *6*, 67−83.

(6) Liu, D.; Wang, Q.; Wu, J.; Liu, Y. A review of sorbents for high-temperature hydrogen sulfide removal from hot coal gas. *Environ. Chem. Lett.* **2019**, *17*, 259−276.

(7) Wu, J.; Liu, D. J.; Zhou, W. G.; Liu, Q. Z.; Huang, Y. J. *High-Temperature H_2S Removal from IGCC Coarse Gas*; Springer: Singapore.

(8) Oh, W.-D.; Lei, J.; Veksha, A.; Giannis, A.; Lisak, G.; Chang, V. W.-C.; Hu, X.; Lim, T.-T. Influence of surface morphology on the performance of nanostructured ZnO-loaded ceramic honeycomb for syngas desulfurization. *Fuel* **2018**, *211*, 591−599.

(9) Liu, Q.; Liu, B.; Liu, Q.; Xu, R.; Xia, H. Lattice substitution and desulfurization kinetic analysis of Zn-based spinel sorbents loading onto porous silicoaluminophosphate zeolites. *J. Hazard. Mater.* **2020**, *383*, 121151−121163.

(10) Su, Y.-M.; Huang, C.-Y.; Chyou, Y.-P.; Svoboda, K. Sulfidation/regeneration multi-cyclic testing of Fe_2O_3/Al_2O_3 sorbents for the high-temperature removal of hydrogen sulfide. *J. Taiwan Inst. Chem. Eng.* **2017**, *74*, 89−95.

(11) Wu, M.; Guo, E.; Li, Q.; Mi, J.; Fan, H. Mesoporous Zn-Fe-based binary metal oxide sorbent with sheet-shaped morphology: Synthesis and application for highly efficient desulfurization of hot coal gas. *Chem. Eng. J.* **2020**, *389*, 123750−123763.

(12) Yazdanbakhsh, F.; Bläsing, M.; Sawada, J. A.; Rezaei, S.; Müller, M.; Baumann, S.; Kuznicki, S. M. Copper exchanged nanotitanate for

high temperature H_2S adsorption. *Ind. Eng. Chem. Res.* **2014**, *53*, 11734−11739.
(13) Liu, D.; Zhou, W.; Wu, J. CuO-CeO_2/ZSM-5 composites for reactive adsorption of hydrogen sulfide at high temperature. *Can. J. Chem. Eng.* **2016**, *94*, 2276−2281.
(14) Liu, D.; Zhou, W.; Wu, J. La_2CuO_4/ZSM-5 sorbents for high-temperature desulphurization. *Fuel* **2016**, *177*, 251−259.
(15) Li, H.; Su, S.; Hu, S.; Xu, K.; Jiang, L.; Wang, Y.; Xu, J.; Xiang, J. Effect of preparation conditions on Mn_xO_y/Al_2O_3 sorbent for H_2S removal from high-temperature synthesis gas. *Fuel* **2018**, *223*, 115−124.
(16) Zhang, F. M.; Liu, B. S.; Zhang, Y.; Guo, Y. H.; Wan, Z. Y.; Subhan, F. Highly stable and regenerable Mn-based/SBA-15 sorbents for desulfurization of hot coal gas. *J. Hazard. Mater.* **2012**, *233*−*234*, 219−227.
(17) Huang, Z. B.; Liu, B. S.; Tang, X. Y.; Wang, X. H.; Amin, R. Performance of rare earth oxide doped Mn-based sorbent on various silica supports for hot coal gas desulfurization. *Fuel* **2016**, *177*, 217−225.
(18) Wang, F.; Liu, B. S.; Zhang, Z. F.; Zheng, S. High-temperature desulfurization of coal gas over Sm doped Mn-based/MSU-S sorbents. *Ind. Eng. Chem. Res.* **2015**, *54*, 8405−8416.
(19) Xia, H.; Liu, B.; Li, Q.; Huang, Z.; Cheung, A. S.-C. High capacity Mn-Fe-Mo/FSM-16 sorbents in hot coal gas desulfurization and mechanism of elemental sulfur formation. *Appl. Catal., B* **2017**, *200*, 552−565.
(20) Chytil, S.; Lind, A.; Vanhaecke, E.; Blekkan, E. A. Preparation and Characterization of Mn $_xO_y$ -Al_2O_3 Sorbents for H_2S Removal from Biomass Gasification Gas. *Energy Proc.* **2012**, *26*, 98−106.
(21) Bakker, W. J. W.; Kapteijn, F.; Moulijn, J. A. A high capacity manganese-based sorbent for regenerative high temperature desulfurization with direct sulfur production conceptual process application to coal gas cleaning. *Chem. Eng. J.* **2003**, *96*, 223−235.
(22) Wang, J.; Liang, B.; Parnas, R. Manganese-based regenerable sorbents for high temperature H_2S removal. *Fuel* **2013**, *107*, 539−546.
(23) Zeng, B.; Li, H.; Huang, T.; Liu, C.; Yue, H.; Liang, B. Kinetic Study on the Sulfidation and Regeneration of Manganese-Based Regenerable Sorbent for High Temperature H_2S Removal. *Ind. Eng. Chem. Res.* **2015**, *54*, 1179−1188.
(24) Suyadal, Y.; Erol, M.; Oğuz, H. Deactivation Model for the Adsorption of Trichloroethylene Vapor on an Activated Carbon Bed. *Ind. Eng. Chem. Res.* **2000**, *39*, 724−730.
(25) Hong, Y. S.; Zhang, Z. F.; Cai, Z. P.; Zhao, X. H.; Liu, B. S. Deactivation Kinetics Model of H_2S Removal over Mesoporous $LaFeO_3$/MCM-41 Sorbent during Hot Coal Gas Desulfurization. *Energy Fuels* **2014**, *28*, 6012−6018.
(26) Hong, Y.-S.; Sin, K.-R.; Pak, J.-S.; Kim, C.-J.; Liu, B.-S. Kinetic Analysis of H_2S Removal over Mesoporous Cu-Mn Mixed Oxide/SBA-15 and La-Mn Mixed Oxide/KIT-6 Sorbents during Hot Coal Gas Desulfurization Using the Deactivation Kinetics Model. *Energy Fuels* **2017**, *31*, 9874−9880.
(27) Ozaydin, Z.; Yasyerli, S.; Dogu, G. Synthesis and activity comparison of copper-incorporated MCM-41-type sorbents prepared by one-pot and impregnation procedures for H_2S removal. *Ind. Eng. Chem. Res.* **2008**, *47*, 1035−1042.
(28) Caglayan, P.; Yasyerli, S.; Ar, I.; Dogu, G.; Dogu, T. Kinetics of H_2S sorption on manganese oxide and Mn-Fe-Cu mixed oxide prepared by the complexation technique. *Int. J. Chem. React. Eng.* **2006**, *4*, 1−10.
(29) Yasyerli, S. Cerium-manganese mixed oxides for high temperature H_2S removal and activity comparisons with V-Mn, Zn-Mn, Fe-Mn sorbents. *Chem. Eng. Process.* **2008**, *47*, 577−584.
(30) Sadegh-Vaziri, R.; Babler, M. U. Removal of Hydrogen Sulfide with Metal Oxides in Packed Bed Reactors-A Review from a Modeling Perspective with Practical Implications. *Appl. Sci.* **2019**, *9*, 5316−5339.
(31) Montogomery, D. C. *Design and analysis of experiments*, 8th ed.; John Wiley & Sons, 2012: New York, United States.
(32) Zheng, X.; Cai, J.; Cao, Y.; Shen, L.; Zheng, Y.; Liu, F.; Liang, S.; Xiao, Y.; Jiang, L. Construction of cross-linked δ-MnO_2 with ultrathin structure for the oxidation of H_2S: Structure-activity relationship and kinetics study. *Appl. Catal., B* **2021**, *297*, 120402−120418.
(33) Chytil, S.; Kure, M.; Lødeng, R.; Blekkan, E. A. On the initial deactivation of Mn_xO_y-Al_2O_3 sorbents for high temperature removal of H_2S from producer gas. *Fuel Process. Technol.* **2015**, *133*, 183−194.
(34) Wang, J.; Guo, J.; Parnas, R.; Liang, B. Calcium-based regenerable sorbents for high temperature H_2S removal. *Fuel* **2015**, *154*, 17−23.

https://doi.org/10.1021/acsomega.1c05243
ACS Omega 2022, 7, 2718−2724